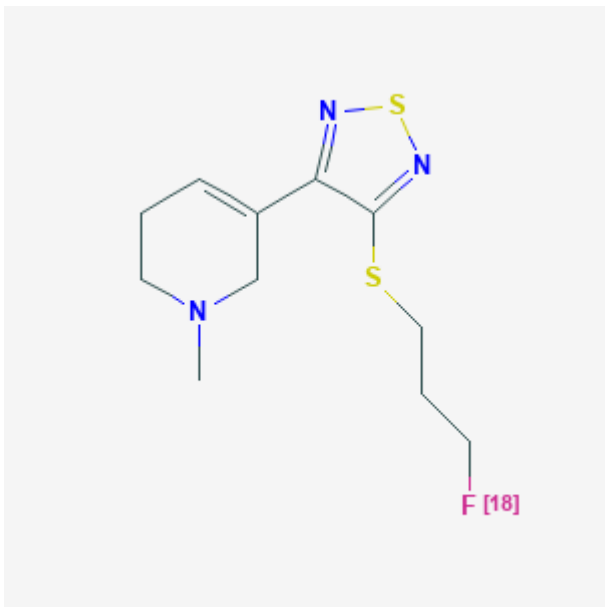


3-(3-(3-[¹⁸F]Flouoropropyl)thio)-1,2,5-thiadiazol-4-yl)-1,2,5,6-tetrahydro-1-methylpyridine

[¹⁸F]FP-TZTP

Kam Leung, PhD[✉]

Created: May 25, 2005; Updated: June 6, 2005.

Chemical name:	3-(3-(3-[¹⁸ F]Flouoropropyl)thio)-1,2,5-thiadiazol-4-yl)-1,2,5,6-tetrahydro-1-methylpyridine	
Abbreviated name:	[¹⁸ F]FP-TZTP	
Synonym:		
Backbone:	Compound	
Target:	Muscarinic M ₂ receptor	
Mechanism:	Receptor binding	
Method of detection:	PET	
Source of signal:	¹⁸ F	
Activation:	No	
Studies:	<ul style="list-style-type: none"> • <i>In vitro</i> • Rodents • Non-human primates • Humans 	
		Click on the above structure for additional information in PubChem .

Background

[PubMed]

The current state of molecular genetics of Alzheimer's disease (AD) focuses on four genes: the β -amyloid precursor protein (β -APP) gene, the presenilin 1 gene, the presenilin 2 gene, and the apolipoprotein E (APOE) gene (2). The ϵ 4 allele of the APOE gene is associated with an increased risk for late-onset AD (>50 years of age). Few of the imaging studies to date have been based on these genetic abnormalities. The characteristic neuropathology is neurofibrillary tangles and amyloid plaques. The result of the phenotypic changes is caused by an alteration in the processing of β -APP favoring the production of the potentially toxic A β 42 protein. Binding

of radioligands to A β 42 protein *in vivo* has been reported (3). There has also been a report on the use of 2-[¹⁸F]fluoro-2-deoxyglucose ([¹⁸F]FDG) in a subpopulation of AD patients with the APOE gene (4), although this is an indirect measure of the phenotype. The authors found changes in FDG distribution before clinical manifestations.

Muscarinic cholinergic M₂ subtype-selective ligands were developed based on the observation that this subtype is lost in the cerebral cortex in AD (5-7). Postmortem quantization of muscarinic subtypes indicated a selective loss of the M₂ subtype in cortical regions, whereas the M₁ subtype was preserved. Thus, an M₂-selective ligand labeled with a positron-emitting radionuclide would allow determination of M₂ subtype density in the living human brain. Several investigators have pursued muscarinic receptor imaging with positron emission tomography (2) and single-photon emission computed tomography (SPECT) (8, 9). Most tracers for cholinergic receptors have not demonstrated subtype selectivity. Alternatively, ligands that are subtype selective *in vitro* typically do not cross the blood-brain barrier (BBB). In addition to muscarinic receptors, ligands for the nicotinic receptors (10, 11) and acetylcholinesterase (12) have been investigated. Acetylcholinesterase (13-15) has been a target for radioligand development because its levels also change in AD. In addition, the vesicular acetylcholine (ACh) transporter has been studied recently in patients with AD using [¹²³I]iodobenzovesamicol (12). The probe for acetylcholinesterase (*N*-[¹¹C]methylpiperidin-4-yl propionate, [¹¹C]PMP) has been used in AD patients and found to show a decrease that is more uniform and broadly distributed than the focal defects found with [¹⁸F]FDG (12). 3-((3-(3-fluoropropyl)thio)-1,2,5-thiadiazol-4-yl)-1,2,5,6-tetrahydro-1-methylpyridine (FP-TZTP), a muscarinic agonist based on a series of non-fluorinated analogs first proposed by Sauerberg *et al.* (16), was radiolabeled with the positron-emitting radionuclide ¹⁸F ([¹⁸F]FP-TZTP) (17). [¹⁸F]FP-TZTP was found to be a promising imaging agent for the M₂ system in the brain.

Synthesis

[PubMed]

Nucleophilic fluorination of 3-((3-((3-(methanesulfonyoxy)-propyl)thio)-1,2,5-thiadiazol-4-yl)-1,2,5,6-tetrahydro-1-methylpyridine with K[¹⁸F]F/Kryptofix2.2.2 to form [¹⁸F]FP-TZTP (18). A one-step radiosynthesis of [¹⁸F]FP-TZTP was developed and can also be conducted with an automated synthesis unit. The manual synthesis produced [¹⁸F]FP-TZTP in a radiochemical yield of 23.4% \pm 4.3% (EOS, n = 69) with a specific activity of 117 \pm 54 MBq/ μ mol, 4377 \pm 2011 mCi/ μ mol (EOB, n = 100). The automated synthesis unit provided [¹⁸F]FP-TZTP in a radiochemical yield of 18.8% \pm 2.4% (EOS, n = 25) with a specific activity of 111 \pm 70 MBq/ μ mol, 4112 \pm 2572 mCi/ μ mol (EOB, n = 25) (18).

In Vitro Studies: Testing in Cells and Tissues

[PubMed]

FP-TZTP showed a K_i of 7.4 nM for M₁ and 2.2 nM for M₂. It did not bind to M₃ receptors or other biogenic amine receptors (19).

Rat hepatocytes were incubated with [¹⁸F]FP-TZTP with (carrier-added) or without (no-carrier-added) the addition of 20 μ g of unlabeled FP-TZTP. The time course of metabolites from the sequential analysis of the no-carrier-added experiment revealed that the parent compound was nearly consumed within 2 h, concomitant with the formation of seven radiolabeled metabolites. The carrier-added experiment showed slower metabolism. The 30-min, carrier-added sample was selected for identification of the metabolites by liquid chromatography tandem mass spectrometry (LC/MS/MS). Structures were confirmed for all compounds by comparison of retention time and MS/MS fragmentation with the synthesized standards. N-Oxidation provided the major radioactive metabolite. Other major metabolites were formed from sulfur oxidation, demethylation of the tertiary amine, and dehydrogenation of the tetrahydropyridine ring, respectively. In addition to the major

metabolites of FP-TZTP identified above, two more polar radioactivity peaks were found in the radiochromatogram. The peak eluting at the solvent front was identified as [¹⁸F]fluoride. The remaining peak was unidentified based on the MS/MS data. Compared with rat hepatocytes, human hepatocytes produced a similar metabolite profile. The N-oxide was also the major metabolite identified by LC/MS and radiochromatography. However, N-oxidation metabolites were not obtained with the same dominance as observed in rat hepatocytes. Demethylation and S-oxidation metabolites were also produced by human hepatocytes. The ring oxidation metabolite and its hydroxylated analog were also found in human hepatocytes (20).

Animal Studies

Rodents

[PubMed]

Metabolism of [¹⁸F]FP-TZTP *in vivo* is rapid (21). In rat, only 5% of plasma radioactivity was in the parent compound by 15 min after injection. One metabolite was almost as lipophilic as the parent compound, as measured by TLC, suggesting that it might cross the BBB. However, the parent compound was found to represent >95% of extracted radioactivity in rat brain through 30 min and >90% at 45 and 60 min.

Autoradiography using no-carrier-added [¹⁸F]FP-TZTP confirmed the uniform distribution of radioactivity characteristic of the M₂ pattern of localization (22). Coinjection of a muscarinic agonist, (3-(propylthio)-1,2,5-thiadiazol-4-yl)-tetrahydro-1-methyl-pyridine (P-TZTP), at 5, 50, and 500 nmol inhibited [¹⁸F]FP-TZTP uptake in a dose-dependent manner at 1 hour after i.v. injection. The difference in brain regions between each dose level was significant ($p < 0.01$), except for the 5-nmol value in the medulla ($p < 0.06$). The brain distribution of the agonist [¹⁸F]FP-TZTP was unaffected by coinjection of 5, 50, or 500 nmol of the antagonist R-3-quinuclidinyl-R-4-[¹²³I]iodobenzilate (RR-IQNB). Likewise, the distribution of [¹⁸F]FP-TZTP was unaffected by co-injection of 500 nmol of the M₂-selective antagonist RS-FMeQNB except in the cerebral cortex and hippocampus, where the difference was significant ($p < 0.03$). Binding in the heart was low by 15 min; therefore, earlier time points were studied. At 5 min, 55% inhibition of uptake in the heart was observed with co-injection of P-TZTP.

Biodistribution of [¹⁸F]FP-TZTP was studied in WT mice and in genetically engineered mice lacking functional M₁, M₂, M₃, or M₄ muscarinic receptors (23). Using *ex vivo* autoradiography, the regional brain localization of [¹⁸F]FP-TZTP in M₂ knockout (M₂ KO) mice was significantly decreased (51.3% to 61.4%; $p < 0.01$) compared with the WT mice in amygdala, brain stem, caudate putamen, cerebellum, cortex, hippocampus, hypothalamus, superior colliculus, and thalamus. In similar studies with M₁ KO, M₃ KO, and M₄ KO mice compared with WT mice, [¹⁸F]FP-TZTP uptake in the same brain regions was not significantly decreased. [¹⁸F]FP-TZTP preferentially labels M₂ receptors *in vivo* because large decreases in [¹⁸F]FP-TZTP brain uptake were seen only in M₂ KO *versus* WT mice,.

Other Non-Primate Mammals

[PubMed]

No publication is currently available.

Non-Human Primates

[PubMed]

PET studies of isoflurane-anesthetized rhesus monkeys were performed to assess the *in vivo* behavior of [¹⁸F]FP-TZTP (24). Control studies were performed to characterize tracer kinetics and to choose an appropriate

mathematical model for the *in vivo* behavior of the tracer. Metabolite correction of the arterial input data was performed using TLC. The parent compound represented $48 \pm 9\%$, $28 \pm 6\%$, and $13 \pm 3\%$ plasma radioactivity at 15, 30, and 90 min, respectively. [^{18}F]FP-TZTP time-activity curves in brain were well described by a one-compartment model with three parameters: uptake rate constant K_1 , total volume of distribution V and a global brain-to-blood time delay Δt . Tracer uptake in the brain was rapid, with K_1 values of 0.4 to 0.6 ml/min/ml in gray matter.

The volume of distribution V represents total tracer binding (free, nonspecifically bound, and specifically bound). V values were similar (22-26 ml/ml) in cortical regions, basal ganglia, and thalamus but were significantly lower (16 ml/ml, $p < 0.01$) in the cerebellum. In comparing these V values with the receptor distribution reported for rat and monkey, there was an excellent match with the M_2 distribution. In rat, the concentrations of M_2 receptors in cortical structures, basal ganglia, and thalamus are highly uniform and are approximately 50% lower in cerebellum (25). In rhesus monkey, the distributions of M_2 receptors are also uniform in cortex, basal ganglia, and thalamus (26). This pattern is unlike that of M_1 receptors (the muscarinic subtype to which this tracer shows threefold lower *in vitro* affinity) for which basal ganglia > cortex > thalamus (26, 27).

Preblocking studies were used to measure nonspecific binding. Pre-administering 200-400 nmol/kg of nonradioactive FP-TZTP produced a dramatic reduction in total binding of about 50% in cerebellum and 60-70% in other gray matter regions. Similar blockade was seen in analogous rat studies (19). This reduction was highly significant in all regions, and the regional distribution of V values after pre-blocking became nearly uniform. In addition to preblocking studies, displacement of [^{18}F]FP-TZTP with 80 nmol/kg of FP-TZTP at 45 min after injection caused a distinct increase in net efflux with decreases of 20%, 36%, and 41% in cerebellum, cortex, and thalamus, respectively (21). The sensitivity of [^{18}F]FP-TZTP binding to changes in brain ACh was assessed by administering physostigmine, an acetylcholinesterase inhibitor, by i.v. infusion beginning 30 min before tracer injection. Physostigmine produced a 35% reduction in cortical-specific binding ($p < 0.05$), consistent with increased competition from ACh.

[^{18}F]FP-TZTP was used to assess the muscarinic effects of procaine (28), which has been used previously to induce emotional and psychosensory experiences in healthy controls and patients with mood disorders (29). With paired monkey studies on the same day using continuous infusion of procaine (0.016-0.5 mg/kg/min), [^{18}F]FP-TZTP-specific binding was globally blocked up to 90% in a dose-dependent manner with an EC_{50} of about 0.063 mg/kg/min. This suggested a role for M_2 receptors in procaine-induced effects in consistent with a cholinergic hypothesis of mood regulation.

Human Studies

[PubMed]

[^{18}F]FP-TZTP dosimetry in humans was determined from its biodistribution in monkeys by i.v. of 93-130 MBq (2.5-3.5 mCi) [^{18}F]FP-TZTP (30). There was early accumulation of activity in liver and kidney, with subsequent appearance of activity in gallbladder and urine, reflecting pathways for tracer excretion. The effective dose equivalent was 0.023 mSv/MBq (85 mrem/mCi). The critical organ was urinary bladder (0.073 mGy/MBq, 269 mrad/mCi), followed by pancreas (0.047 mGy/MBq, 173 mrad/mCi), gallbladder (0.040 mGy/MBq, 147 mrad/mCi), and brain (0.023 mGy/MBq, 86 mrad/mCi).

[^{18}F]FP-TZTP PET was studied in healthy volunteers (31). In plasma, the parent compound represented $68 \pm 8\%$, $41 \pm 9\%$, and $14 \pm 4\%$ of radioactivity at 20, 40, and 120 min, respectively. The plasma-free fraction was $5.9 \pm 1.2\%$. A model with one tissue compartment produced an excellent fit for the full 120 min of data, so that the additional parameters of a two-compartment model were unidentifiable. K_1 values in gray matter regions were high, 0.36 to 0.56 ml/min/ml, and showed excellent correlation with cerebral blood flow. V values, representing

total tissue binding, were similar in cortical regions, basal ganglia, and thalamus but were significantly higher ($p < 0.01$) in amygdala. Unlike the results in the monkey, binding in the cerebellum was similar to that in the cerebral cortex.

In the first clinical studies, an age-related increase in M₂ receptor binding potential was observed using [¹⁸F]FP-TZTP and PET in normal subjects (32). There was a significant increase not only in the average volume of distribution but also for variance in the older subjects. This infers that other aspects of the systems biology were coming into play, and therefore the data should be modeled by a more complex set of equations. The increase in variance for the volume of distribution was caused by using age discrimination only. This suggested the possibility that the age-related changes might be associated with a specific genotype, such as the APOE-ε4 allele. In the following study, Cohen *et al.* (33) found that the gray matter distribution volume for [¹⁸F]FP-TZTP was significantly higher in the APOE-ε4-positive normal subjects than in the APOE-ε4-negative normal subjects, whereas there were no differences in global cerebral blood flow. Given that [¹⁸F]FP-TZTP measures the muscarinic system rather than only receptor density because of its agonist properties, changes in receptor binding affinity attributable to changes in G protein binding and competition with ACh at the muscarinic receptor can be monitored. The increased volume of distribution in elderly normal subjects with APOE-ε4 positivity may be because of a decreased concentration of ACh in the synapse, which would lead to higher binding of [¹⁸F]FP-TZTP. This type of competition was shown to be possible in the studies in monkeys using physostigmine (21). As a result, the use of [¹⁸F]FP-TZTP can be considered an *in vivo* measurement of muscarinic systems biology, rather than of receptor density alone.

Supplemental Information

[Disclaimers]

Synthesis Protocol A

Synthesis Protocol B

Preclinical Pharmacology

NIH Support

Intramural Research Program

References

1. Slavicek J.M., Hayes-Plazolles N. *The Lymantria dispar nucleopolyhedrovirus contains the capsid-associated p24 protein gene.* . Virus Genes. 2003;26(1):15–8. PubMed PMID: 12680688.
2. St George-Hyslop P.H., Petit A. *Molecular biology and genetics of Alzheimer's disease.* . C R Biol. 2005;328(2):119–30. PubMed PMID: 15770998.
3. Bacskai B.J. et al. *Imaging amyloid-beta deposits in vivo.* . J Cereb Blood Flow Metab. 2002;22(9):1035–41. PubMed PMID: 12218409.
4. Frey K.A., Minoshima S., Kuhl D.E. *Neurochemical imaging of Alzheimer's disease and other degenerative dementias.* . Q J Nucl Med. 1998;42(3):166–78. PubMed PMID: 9796365.
5. Aubert I. et al. *Comparative alterations of nicotinic and muscarinic binding sites in Alzheimer's and Parkinson's diseases.* . J Neurochem. 1992;58(2):529–41. PubMed PMID: 1729398.
6. Quirion R. et al. *Muscarinic receptor subtypes in human neurodegenerative disorders: focus on Alzheimer's disease.* . Trends Pharmacol Sci. 1989. Suppl.:80–4. PubMed PMID: 2694529.
7. Rodriguez-Puertas R. et al. *Autoradiographic distribution of M1, M2, M3, and M4 muscarinic receptor subtypes in Alzheimer's disease.* . Synapse. 1997;26(4):341–50. PubMed PMID: 9215593.

8. Freo U.et al. *A short review of cognitive and functional neuroimaging studies of cholinergic drugs: implications for therapeutic potentials.* . J Neural Transm. 2002;109(5-6):857–70. PubMed PMID: 12111473.
9. Maziere M. *Cholinergic neurotransmission studied in vivo using positron emission tomography or single photon emission computerized tomography.* . Pharmacol Ther. 1995;66(1):83–101. PubMed PMID: 7630931.
10. Gatley S.J.et al. *In vitro and ex vivo autoradiographic studies of nicotinic acetylcholine receptors using [18F]fluoronochloroepibatidine in rodent and human brain.* . Nucl Med Biol. 1998;25(5):449–54. PubMed PMID: 9720662.
11. Horti A.G.et al. *2-[18F]Fluoro-A-85380, an in vivo tracer for the nicotinic acetylcholine receptors.* . Nucl Med Biol. 1998;25(7):599–603. PubMed PMID: 9804040.
12. Kuhl D.E.et al. *In vivo mapping of cerebral acetylcholinesterase activity in aging and Alzheimer's disease.* . Neurology. 1999;52(4):691–9. PubMed PMID: 10078712.
13. Kilbourn M.R.et al. *In vivo studies of acetylcholinesterase activity using a labeled substrate, N-[11C]methylpiperdin-4-yl propionate ([11C]PMP).* . Synapse. 1996;22(2):123–31. PubMed PMID: 8787128.
14. Namba H.et al. *In vivo measurement of acetylcholinesterase activity in the brain with a radioactive acetylcholine analog.* . Brain Res. 1994;667(2):278–82. PubMed PMID: 7697367.
15. Tavitian B.et al. *In vivo visualization of acetylcholinesterase with positron emission tomography.* . Neuroreport. 1993;4(5):535–8. PubMed PMID: 8513134.
16. Sauerberg Pet al. *Novel functional M1 selective muscarinic agonists. Synthesis and structure-activity relationships of 3-(1,2,5-thiadiazolyl)-1,2,5,6-tetrahydro-1-methylpyridines.* . J Med Chem. 1992;35(12):2274–83. PubMed PMID: 1613751.
17. Eckelman W.C. *Radiolabeled muscarinic radioligands for in vivo studies.* . Nucl Med Biol. 2001;28(5):485–91. PubMed PMID: 11516692.
18. Kiesewetter D.O., Vuong B.K., Channing M.A. *The automated radiosynthesis of [18F]FP-TZTP.* . Nucl Med Biol. 2003;30(1):73–7. PubMed PMID: 12493545.
19. Kiesewetter D.O.et al. *Preparation of 18F-labeled muscarinic agonist with M2 selectivity.* . J Med Chem. 1995;38(1):5–8. PubMed PMID: 7837240.
20. Ma Y.et al. *Identification of metabolites of fluorine-18-labeled M2 muscarinic receptor agonist, 3-(3-[(3-fluoropropyl)thio]-1,2,5-thiadiazol-4-yl)-1,2,5,6-tetrahydro-1-methylpyridine, produced by human and rat hepatocytes.* . J Chromatogr B Analyt Technol Biomed Life Sci. 2002;766(2):319–29. PubMed PMID: 11824820.
21. Kiesewetter D.O.et al. *In vivo muscarinic binding of 3-(alkylthio)-3-thiadiazolyl tetrahydropyridines.* . Synapse. 1999;31(1):29–40. PubMed PMID: 10025681.
22. Kiesewetter D.O.et al. *Using single photon emission tomography (SPECT) and positron emission tomography (PET) to trace the distribution of muscarinic acetylcholine receptor (MACHR) binding radioligands.* . Life Sci. 1999;64(6-7):511–8. PubMed PMID: 10069517.
23. Jagoda E.M.et al. *Regional brain uptake of the muscarinic ligand, [18F]FP-TZTP, is greatly decreased in M2 receptor knockout mice but not in M1, M3 and M4 receptor knockout mice.* . Neuropharmacology. 2003;44(5):653–61. PubMed PMID: 12668051.
24. Carson R.E.et al. *Muscarinic cholinergic receptor measurements with [18F]FP-TZTP: control and competition studies.* . J Cereb Blood Flow Metab. 1998;18(10):1130–42. PubMed PMID: 9778190.
25. Li M.et al. *Distribution of m2 muscarinic receptors in rat brain using antisera selective for m2 receptors.* . Mol Pharmacol. 1991;40(1):28–35. PubMed PMID: 1857338.
26. Flynn D.D., Mash D.C. *Distinct kinetic binding properties of N-[3H]-methylscopolamine afford differential labeling and localization of M1, M2, and M3 muscarinic receptor subtypes in primate brain.* . Synapse. 1993;14(4):283–96. PubMed PMID: 8248852.
27. Wall S.J.et al. *Production of antisera selective for m1 muscarinic receptors using fusion proteins: distribution of m1 receptors in rat brain.* . Mol Pharmacol. 1991;39(5):643–9. PubMed PMID: 2034236.
28. Benson B.E.et al. *A potential cholinergic mechanism of procaine's limbic activation.* . Neuropsychopharmacology. 2004;29(7):1239–50. PubMed PMID: 14997171.

29. Ketter T.A.et al. *Anterior paralimbic mediation of procaine-induced emotional and psychosensory experiences.* . Arch Gen Psychiatry. 1996;53(1):59–69. PubMed PMID: 8540778.
30. Herscovitch P, Kiesewetter D.O., Carson R.E. *Biodistribution and radiation dose estimates for [F-18] fluoropropyl-TZTP, a new muscarinic cholinergic ligand.* . . J Nucl Med. 1998;39:85P.
31. Carson R.E.et al. *Evaluation of a new F-18 labeled analog of the 5-HT1A antagonist WAY 100635 for PET.* . J Nucl Med. 1998;39:135P.
32. Podruchny T.A.et al. *In vivo muscarinic 2 receptor imaging in cognitively normal young and older volunteers.* . Synapse. 2003;48(1):39–44. PubMed PMID: 12557271.
33. Cohen R.M.et al. *Higher in vivo muscarinic-2 receptor distribution volumes in aging subjects with an apolipoprotein E-epsilon4 allele.* . Synapse. 2003;49(3):150–6. PubMed PMID: 12774299.